# Sign Dependence of MCPL spectra on Type and Position of Substituent Groups of Pyrene and Phenanthrene Derivatives

| | |
|---|---|
| Journal: | *Physical Chemistry Chemical Physics* |
| Manuscript ID | CP-COM-01-2021-000259.R1 |
| Article Type: | Communication |
| Date Submitted by the Author: | 19-Feb-2021 |
| Complete List of Authors: | Hara, Nobuyuki; Kinki University<br>Kitahara, Maho; Kindai University<br>Sugimura, Takaharu; Kindai University<br>Toda, Hayato; Kindai University Faculty of Science and Engineering Graduate School of Science and Engineering Department of Science Mathematics Course<br>Shizuma, Motohiro; Osaka Research Institute of Industrial and Scientific Technology, Department of Biochemistry<br>Ito, Araki; Kindai University<br>Miyasaka, Makoto; Tokyo Denki University, Department of Applied Chemistry<br>FUJIKI, Michiya; Nara Institute of Science and Technology, Division of Materials Science;<br>Imai, Yoshitane; Kinki University, Department of Applied Chemistry |
| | |

COMMUNICATION

# Sign Dependence of MCPL spectra on Type and Position of Substituent Groups of Pyrene and Phenanthrene Derivatives

Nobuyuki Hara,[a] Maho Kitahara,[a] Takaharu Sugimura,[a] Hayato Toda,[a] Motohiro Shizuma,[b] Akari Ito,[c] Makoto Miyasaka,[c] Michiya Fujiki,[d] and Yoshitane Imai*[a]

Received 00th January 20xx,
Accepted 00th January 20xx

DOI: 10.1039/x0xx00000x

***Diamagnetic achiral pyrene and phenanthrene derivatives substituted with electron-donating hydroxyl/methoxy groups and electron-withdrawing carboxylic acid groups exhibited clear magnetic circularly polarised luminescence (MCPL) spectra at 360–410 nm in dilute solvents upon the application of N-up and S-up Faraday geometries under an external magnetic field of 1.6 T. Their MCPL signs were also susceptible upon application of the same Faraday geometry.***

Recently, numerous chiral organic compounds, supramolecular complexes, organometallic substances, and helical polymers have been designed to achieve a high-performance circularly polarised luminescence (CPL) with relatively high dissymmetry ratios ($g_{\mathrm{CPL}}$) in the near-UV, visible, and near-infrared regions.[1,2] These luminophores have the potential to enable the development of sophisticated photonic and optoelectronic devices.[1-3] Nevertheless, luminophores with suitable stereogenic elements (centres, plane- or axial-dissymmetry elements, etc.) are required to afford a CPL with controllable handedness.

The application of an external static magnetic field is a versatile physical technique that can generate ambidextrous chiroptical signals from achiral substances. This novel approach relies on Faraday's discovery that a static magnetic field can induce the ambidextrous magnetic optical rotation (MOR) of lead-containing glass in its ground state (GS). The MOR depended on the Faraday geometry, in which north (N)-up or south (S)-up magnetic fields are parallel to the incident light beam. This magneto-optical phenomenon of certain substances is known as the Faraday effect.

Recently, the Faraday effect has been employed to generate magnetic circularly polarised luminescence (MCPL) signals from paramagnetic inorganic substances (e.g., $Eu^{3+}$, $Tb^{3+}$, $Pr^{3+}$, and $Cu^{+}$) in their excited state (ES) with a Faraday geometry.[4] However, most studies use only one Faraday geometry between N-up and S-up ones because it is difficult to simultaneously configure both N-up and S-up geometries.

These ambidextrous MOR experiments by Faraday, in addition to recent MCPL experiments using one of two Faraday geometries, led us to conclude that ES-diamagnetic achiral pyrenes (**Pys**) with and without a hydroxyl group exhibit mirror symmetric MCPL in dilute fluidic and solidified solutions at 25 °C upon the application of both N-up and S-up geometries under an external field of 1.6 T (originating from a palm-sized permanent magnet). The application of N-up and S-up geometries is only possible by alternating the position of the magnet, which is placed in the CPL sample compartment with a 0° forward scattering angle of the incident beam. Interestingly, sign inversion took place in the resulting MCPL due to the peripheral position of the hydroxyl group in the **Py** ring. As expected, the MCPL spectral sign inverts with a change in the Faraday geometry; i.e., the MCPL handedness at the N-up geometry is opposite to that at the S-up geometry.[5]

However, it is important to determine whether the peripheral position-dependent MCPL sign inversion is specific for **Pys** or if it is a general tendency displayed by all fused aromatic systems with circular and arc-shaped topologies. Thus, we experimentally studied the MCPL characteristics of six **Py** derivatives with a circular π-network and two phenanthrene (**Phe**) derivatives with an arc-shaped π-network. Electron-donating (ED, hydroxy and methoxy for **1a–1b**, **2a–2b**, and **3a–3b**) and electron-withdrawing (EWD, carboxylic acid for **1c**, **2c**, and **3c**) groups were substituted at the 1- and 2-positions of the **Py** rings and the 3-position of the **Phe** rings (Fig. 1).

Herein, we demonstrate that the photoexcited **Py** and **Phe** derivatives in dilute organic solvents at 25 °C demonstrate clear mirror-symmetric MCPL spectra in response to N-up and S-up geometries. In addition, the MCPL sign inverts from the ED to EWD groups of **Py** and **Phe** at the same N-up (or S-up) geometry, while 1- and 2-substituted **Pys** display opposite MCPL handedness. Furthermore, the MCPL handedness inverts by

---

*[a] Department of Applied Chemistry, Faculty of Science and Engineering, Kindai University, 3-4-1 Kowakae, Higashi-Osaka, Osaka 577-8502, Japan. E-mail: y-imai@apch.kindai.ac.jp.*

*[b] Department of Biochemistry, Osaka Research Institute of Industrial Science and Technology, 1-6-50 Morinomiya, Joto-ku, Osaka 536-8553, Japan*

*[c] Department of Applied Chemistry, School of Engineering Tokyo Denki University, 5 Senju-Asahi-cho, Adachi-ku, Tokyo 120-8551, Japan*

*[d] Graduate School of Materials Science, Nara Institute of Science and Technology, Takayama, Ikoma, Nara 630-0192, Japan*

*† Electronic Supplementary Information (ESI) available: Experimenatal conditions, chemicals, instrumentations, and MCPL and UV-Vis absorption spectra of luminophores studied here. See DOI: 10.1039/c000000x/.*

changing the substituent (from ED to EWD) in 3-substituted (phenanthrenes) **Phes**, and regardless of the substituent positions, the absolute MCPL magnitudes of the **Pys** bearing ED substituents are slightly larger than those of the **Pys** bearing EWD substituents. Among all **Py** derivatives tested, the unsubstituted **Py** affords the largest MCPL magnitude.[5b]

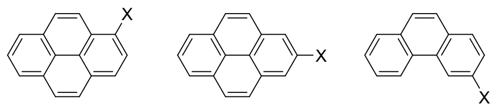

1a, X = OH
1b, X = OMe
1c, X = COOH

2a, X = OH
2b, X = OMe
2c, X = COOH

3a, X = OH
3b, X = OMe
3c, X = COOH

**Fig. 1.** Achiral pyrene (**Py**) and phenanthrene (**Phe**) units substituted with electron donating (ED) and electron withdrawing (EWD) groups.

Six **Py** derivatives bearing ED and EWD groups, **1a–1c**, were purchased from Tokyo Chemical Industry Co., Ltd., while **2a–2c** were prepared following a previously reported method[5] (Schemes S1 and S2 in the SI). In addition, three **Phe** derivatives were employed, where **3a** and **3b** were synthesised as described in the SI (Schemes S3 and S4), while **3c** was purchased from Sigma-Aldrich (Tokyo, Japan).

The MCPL and the corresponding photoluminescence (PL) spectra of **1–3** were simultaneously obtained at N-up and S-up geometries under an external magnetic field of 1.6 T. Regardless of the substituents present, if any, the **Py** family demonstrates a clear MCPL spectra at the N-up geometry under the 1.6 T magnetic field in a dilute chloroform ($CHCl_3$) solution (Fig. 2).

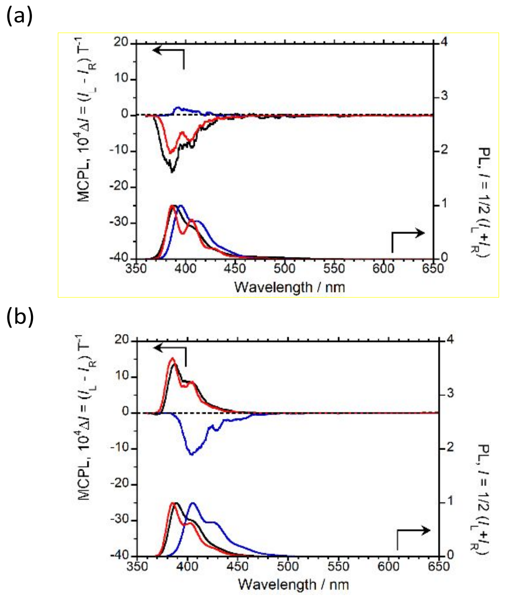

**Fig. 2**. MCPL (upper panel) and PL (lower panel) spectra of the (a) **1a** (black),[5b] **1b** (red), and **1c** (blue) luminophores, and the (b) **2a** (black),[5b] **2b** (red), and **2c** (blue) luminophores in $CHCl_3$ ($1.0 \times 10^{-4}$ M) at the N-up geometry under a 1.6 T magnetic field.

The maximum wavelength ($\lambda_{MCPL}$) of the MCPL spectra was between 384 and 405 nm, corresponding to the 0–0′ band of the monomeric **Py** species. As expected, the MCPL handedness changed at the 1.6 T S-up geometry, indicating that a change in the Faraday geometry induces a sign inversion in the MCPL of these **Pys**. As a result, regardless of the substituents present, all **Pys** demonstrated N-up-/S-up-dependent mirror symmetrical MCPL spectra (Figs. S10–S27, in the SI).

The MCPL handedness of the **Pys** substituted with ED (hydroxy for **1a** and **2a** and methoxy for **1b** and **2b**) and EWD (carboxy for **1c** and **2c**) groups was found to be different. In addition, the 1- and 2-peripheral positions show opposite MCPL spectral signs, i.e., the (−)-sign MCPL for **1a** and **1b** and the (+)-sign for **1c** in 1-**Pys**, while in contrast, the (−)-sign for **2c** and the (+)-sign for **2a** and **2b** in 2-**Pys** when the same N-up geometry is applied.

The dissymmetry ratio ($g_{MCPL}$, T$^{-1}$) of MCPL can be expressed as $g_{MCPL} = (I_L - I_R)/[(I_L + I_R)/2]$ per Tesla, where $I_L$ and $I_R$ are the intensities of the left- and right-handed MCPL, respectively, upon excitation with unpolarised incident light.

The value of $g_{MCPL}$ as a function of the wavelength and at a specific $\lambda_{MCPL}$ are plotted in Fig. 3 and summarised in Table 1, respectively. In the case of 1-**Pys**, the ED groups boost the $|g_{MCPL}|$ value five-fold relative to the EWD group: $1.1 \times 10^{-3}$ T$^{-1}$ for **1b** while $0.23 \times 10^{-3}$ T$^{-1}$ for **1c**. On the other hand, in the case of 2-**Py,** ED and EWD groups had little effect on the $|g_{MCPL}|$ value, i.e., $1.5 \times 10^{-3}$ T$^{-1}$ for **2b** and $1.2 \times 10^{-3}$ T$^{-1}$ for **2c**.

**Table 1.** MCPL characteristics of dilute solutions of **1a–1c, 2a–2c**, **3a–3c**, and the corresponding unsubstituted **Pys** in $CHCl_3$ ($1.0\times10^{-4}$ M) and **Phes** in THF ($1.0\times10^{-3}$ M) at the N-up Faraday geometry under a magnetic field of 1.6 T.

| Entry | Solv. | MCPL luminophore | $\lambda_{MCPL}$ / nm | $g_{MCPL}$ / $10^{-3}$ T$^{-1}$ |
|---|---|---|---|---|
| **1**[5b] | $CHCl_3$ | **1a** | 388 | −1.4 |
| **2** | $CHCl_3$ | **1b** | 384 | −1.1 |
| **3** | $CHCl_3$ | **1c** | 393 | $+0.2_4$ |
| **4**[5b] | $CHCl_3$ | **2a** | 388 | +1.4 |
| **5** | $CHCl_3$ | **2b** | 386 | +1.5 |
| **6** | $CHCl_3$ | **2c** | 405 | −1.2 |
| **7** | THF | **3a** | 380 | $-0.9_6$ |
| **8** | THF | **3b** | 377 | $-0.7_8$ |
| **9** | THF | **3c** | 369 | $+0.6_5$ |
| **10**[5b] | $CHCl_3$ | **Py** | 374 | −8.2 |
| **11**[6] | THF | **Phe** | 349 | −1.0 |

In addition, we evaluated the MCPL and PL characteristics of **2a**–**2c** in $CHCl_3$ solution at a higher concentration ($1.0 \times 10^{-2}$ M) to verify the excimer-origin MCPL and PL spectra (Figs. S16, S20, and S24 in the SI). Significant redshifts were observed in the MCPL signals at the 0–0′ band; however, no clear excimer-origin MCPL signals were found at ~450–500 nm. These MCPL signals may arise from the presence of *J*-type slip-stacked dimeric and/or higher associated species in the GS. The $g_{MCPL}$ values for **2a**, **2b**, and **2c** at the N-up geometry were determined to be $1.2 \times 10^{-3}$, $1.2 \times 10^{-3}$, and $2.8 \times 10^{-3}$ T$^{-1}$, respectively. Signals corresponding to the GS-dimeric and/or associated species of **Py**s may be observed when the corresponding ES-species are perturbed by the external magnetic field.

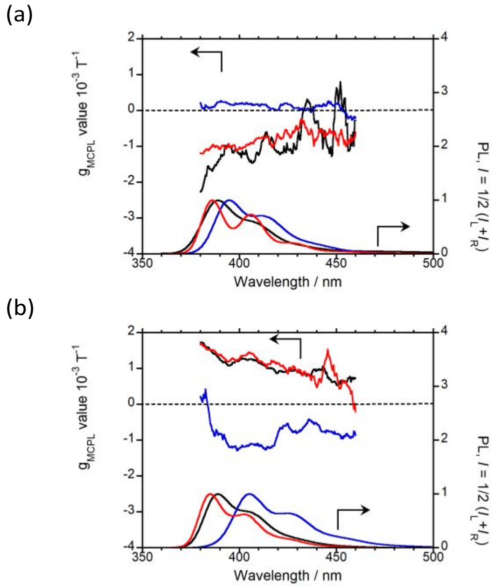

**Fig. 3**. The value of $g_{\mathrm{MCPL}}$ as a function of the wavelength associated with the PL spectra of (a) **1a** (black), **1b** (red), and **1c** (blue), and (b) **2a** (black), **2b** (red), and **2c** (blue) in $CHCl_3$ ($1.0 \times 10^{-4}$ M) at the N-up Faraday geometry under a 1.6 T magnetic field.

All **Phe** derivatives of **3a–3c** in solution of THF were found to exhibit mirror symmetric MCPL spectra between 340 and 400 nm at both the N-up and S-up geometries (Figs. S28–S36 in the SI). Although their $|g_{\mathrm{MCPL}}|$ values ($0.77 \times 10^{-3}$ $T^{-1}$ for **3a**, $0.78 \times 10^{-3}$ $T^{-1}$ for **3b**, $0.65 \times 10^{-3}$ $T^{-1}$ for **3c**) are similar, the MCPL spectral signs of **3a/3b** and **3c** are different at the same N-up geometry. It should be noted that **3c** is scarcely soluble in $CHCl_3$ (Fig. 4).

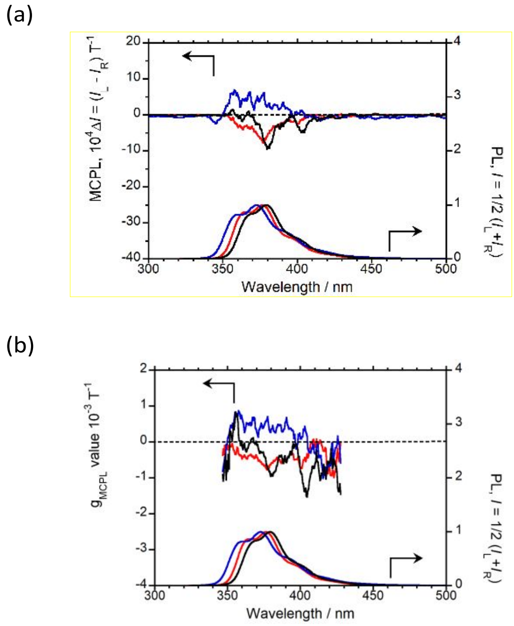

**Fig. 4**. (a) MCPL (upper panel) and PL (lower panel) spectra of **3a** (black), **3b** (red), and **3c** (blue), and (b) the $g_{\mathrm{MCPL}}$ as a function of wavelength of **3a** (black), **3b** (red), and **3c** (blue) in THF ($1.0 \times 10^{-3}$ M) at the N-up geometry under a 1.6 T magnetic field.

Then, for theoretical analysis, we proposed an empirical relationship between the $g_{MCPL}$ values of the **Pys** and **Phes** as functions of the Hammett parameters, including $\delta_p$ and $\delta_m$, to determine the degree of electronic and resonance effects in the ED and EWD groups of the substituted benzene derivatives[7] (Fig. 5).

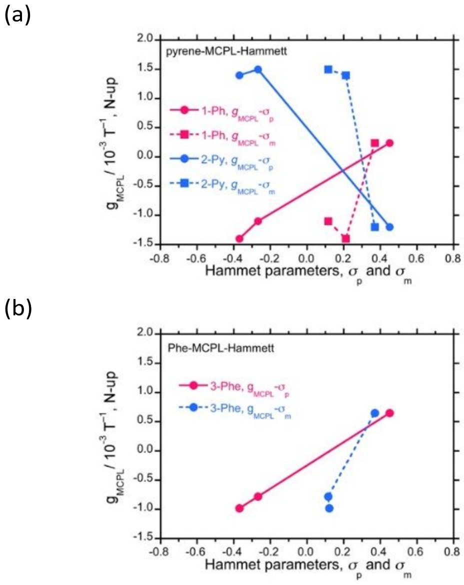

**Fig. 5**. Relationship between the $g_{\mathrm{MCPL}}$ values and the Hammett parameters ($\delta_p$ and $\delta_m$) for (a) **1-Py** and **2-Py;** $\delta_p$ (red) and $\delta_m$ (blue), and for (b) **3-Phe;** $\delta_p$ (red) and $\delta_m$ (blue).

More specifically, the dependence of the MCPL handedness and sign inversion on the nature of the substituents (ED/EWD) and their peripheral positions suggests that the electronic and resonance effects of the aromatic systems may affect the ES[8] . We proposed an empirical relationship between the $g_{\mathrm{MCPL}}$ value and the Hammett parameters ($\delta_p$ and $\delta_m$) for substituted benzene derivatives. The $g_{MCPL}$ values of the **Pys** as functions of $\delta_p$ and $\delta_m$ are plotted in Fig. 5(a). The plot between the $g_{\mathrm{MCPL}}$ of 1-**Pys** and $\delta_p$ shows a good linear correlation (red filled circles), and a similar linear result was observed for 2-**Pys** (blue filled squares), but with the opposite slope. Likewise, a good linear correlation was observed between the $g_{\mathrm{MCPL}}$ values of the 1-/2-substituted **Pys** and $\delta_m$ (red-filled and blue-filled squares). Furthermore, a linear relationship is also observed between the $g_{\mathrm{MCPL}}$ value of the 3-substituted **Phes** and $\delta_p$ and $\delta_m$ (Fig. 5(b)). These findings suggest that the electronic perturbation caused by ED and EWD substituents in the ES-aromatic systems affect the dissymmetry ratio of MCPL. The Hammett parameters for the GS may therefore be related to the degree of spin-orbit coupling in the ES-aromatic systems.

Finally, MCPL properties of **Pys** and **Phes** with ED and EWD group in dimethyl sulfoxide (DMSO) solution state were studied. Although the MCPL wavelength was slightly changed according to the solvent type, MCPL behaver and $g_{\mathrm{MCPL}}$ values were similar to in $CHCl_3$ solution state (Figs. S37–S44, in Table 2 and SI).

**Table 2.** MCPL characteristics of dilute solutions of **1a-1c, 2a-2c** and **3a-3c** in DMSO ($1.0\times10^{-4}$ M) at the N-up Faraday geometry under a magnetic field of 1.6 T.

| Entry | Solv. | MCPL luminophore | $\lambda_{MCPL}$ / nm | $g_{MCPL}$ / $10^{-3}$ $T^{-1}$ |
|---|---|---|---|---|
| **1** | DMSO | **1a** | 409 | $-1.0$ |
| **2** | DMSO | **1b** | 390 | $-0.9_4$ |
| **3** | DMSO | **1c** | 409 | $+0.2_5$ |
| **4** | DMSO | **2a** | 390 | $+0.9_4$ |
| **5** | DMSO | **2b** | 384 | $+1.9$ |
| **6** | DMSO | **2c** | 403 | $-1.5$ |
| **7** | DMSO | **3a** | 373 | $-0.8_5$ |
| **8** | DMSO | **3b** | 361 | $-0.8_6$ |
| **9**[6] | DMSO | **3c** | 374 | $+0.8_3$ |

In summary, we verified that dilute solutions of six **Py** and three **Phe** derivatives bearing electron-donating and electron-withdrawing substituents exhibited mirror-symmetric MCPL in the UV-visible region upon the application of both N-up and S-up Faraday geometries under an external magnetic field of 1.6 T. Notably, the MCPL signs of the **Pys** and **Phes** bearing electron-donating groups differed from those of the corresponding compounds bearing electron-withdrawing groups. Moreover, the MCPL signs of 1- and 2-substituted **Pys** were found to be opposite to one another. Additionally, we interpreted the relationship between the MCPL sign inversion characteristics and the Hammett parameters ($\delta_p$ and $\delta_m$) in a series of substituted benzene derivatives. The present study provides useful insights for the prediction of the MCPL handedness of substituted aromatic systems.

## Acknowledgements

This work was supported by Grants-in-Aid for Scientific Research (KAKENIHI 18K05094, 19H02712, 19H04600, and 20H04678) from MEXT/the Japan Society for the Promotion of Science; the Research Foundation for KDDI (2019-9); the Electrotechnology of Chubu (R-30506); Futaba (2019-6); the Murata Science Foundation (H31-007); the Nippon Sheet Glass Foundation for Materials Science and Engineering (H30-4); and the Yashima Environment Technology Foundation (2019-No9). This work was also supported by JST, CREST (JPMJCR2001), Japan.

## Conflicts of interest

The authors declare no conflict of interest.

## Notes and references

1 (a) H. Tanaka, Y. Inoue, and T. Mori, *ChemPhotoChem*, **2018**, *2*, 386; (b) G. Longhi, E. Castiglioni, J. Koshoubu, G. Mazzeo, and S. Abbate, *Chirality*, **2016**, *28*, 696; (c) E. M. Sánchez-Carnerero, A. R. Agarrabeitia, F. Moreno, B. L. Maroto, G. Muller, M. J. Ortiz, and S. de la Moya, *Chem. Eur. J.* **2015**, *21*, 13488; (d) L. E. Kreno, K. Leong, O. K. Farha, M. Allendorf, R. P. Van Duyne, and J. T. Hupp, *Chem. Rev.* **2012**, *112*, 1105; (e) C. Zhang, Y. S. Zhao, and J. Yao, *New J. Chem.* **2011**, *35*, 973; (f) J. E. Kwon, and S. Y. Park, *Adv. Mater.* **2011**, *23*, 3615; (g) F. Jäkle, *Chem. Rev.* **2010**, *110*, 3985; (h) J. W. Grate, *Chem. Rev.* **2008**, *108*, 726; (i) P. G. Coble, *Chem. Rev.* **2007**, *107*, 402; (j) T. P. I. Saragi, T. Spehr, A. Siebert, T. Fuhrmann-Lieker, and J. Salbeck, *Chem. Rev.* **2007**, *107*, 1011; (k) S.-C. Lo and P. L. Burn, *Chem. Rev.* **2007**, *107*, 1097; (l) K. Walzer, B. Maennig, M. Pfeiffer, and K. Leo, *Chem. Rev.* **2007**, *107*, 1233; (m) H.Y. Wong, W.-S. Lo, K.-H. Yim, and G.-L. Law, *Chem* **2019**, *5*, 3058; and references cited therein.

2 (a) J. L. Ma, Q. Peng and C. H. Qian, *Chem. Eur. J.*, **2019**, *25*, 15441. (b) A. Homberg, E. Brun, F. Zinna, S. Pascal, M. Gorecki, L. Monnier, C. Besnard, G. Pescitelli, L. D. Bari and J. Lacour, *Chem. Sci*., **2018**, *9*, 7043; (c) R. Carr, N. H. Evan and D. Parker, *Chem. Soc. Rev.*, **2012**, *41*, 7673; (d) H. Maeda, Y. Bando, K. Shimomura, I. Yamada, M. Naito, K. Nobusawa, H. Tsumatori and T. Kawai, *J. Am. Chem. Soc.*, **2011**, *133*, 9266; (e) R. Farshchi, M. Ramsteiner, J. Herfort, A. Tahraoui and H. T. Grahn, *Appl. Phys. Lett.* **2011**, *98*, 162508.

3 (a) K. Takaishi, K. Iwachido and T. Ema, *J. Am. Chem. Soc.*, **2020**, *142*, 1774; (b) J. Zhang, L. Yu, R. Gong, M. Li, H. Ren and E. Duan *Energy Fuels* **2020**, *34*, 74; (c) L. Vanden Elzen and T. A. Hopkins, *ACS Sustainable Chem. Eng.*, **2019**, *7*, 16690; (d) J. L. Ma, Q. Peng and C. H. Qian, *Chem. Eur. J.*, **2019**, *25*, 15441. (e) K. Watanabe, A. Taniguchi, D. Kaji, N. Hara, T. Hosoya, A, Kanesaka, T. Harada, H. Nishikawa and Y. Imai, *Tetrahedron*, **2019**, *75*, 2944. (f) S. Nakanishi, N. Hara, R, Kuroda, N, Kuroda, N. Tajima, M. Fujiki and Y. Imai, *Org, Biomol, Chem*., **2018**, *16*, 1097. (g) C. R. Wright, L. V. Elzen and T. A. Hopkins, *J. Phys. Chem. B*., **2018**, *122*, 8730; (h) T, Mizusawa, T, Sato, Y, Kitayama, N, Tajima, M. Fujiki and Y. Imai, *ChemistrySelect*, **2016**, *1*, 3398; (i) T. Kimoto, T. Amako, N. Tajima, R. Kuroda, M. Fujiki, and Y. Imai, *Asian. J. Org. Chem*. **2013**, *2*, 404; (j) T. Ikeda, T. Masuda, T. Hirao, J. Yuasa, H. Tsumatori, T. Kawai and T. Haino, *Chem. Commun*., **2012**, *48*, 6025; (k) A. Satrjio, S. C. J. Meskers and T. M. Swager, *J. Am. Chem. Soc.*, **2006**, *128*, 9030; (l) R. A. van Delden, N. P. M. Huck, J. J. Piet, J. M. Warman, S. C. J. Merkers, H. P. J. M. Dekkers and B. L. Feringa, *J. Am. Chem. Soc.*, **2003**, *125*, 15659.

4 (a) S. Ghidinelli, S. Abbate, G. Mazzeo, L. Paoloni, E. Viola, C. Ercolani, M. P. Donzello, G. Longhi, *Chirality*, **2020**, *32*, 808; (b) Y. Imai, *Symmetry*, **2020**, *12*, 1786. (c) E. L. Iechenko, *Phys. Solid. State*, **2018**, *60*, 1514; (d) T. Wu, J. Kapitan, V. Andrushchenko and P. Bour, *Anal. Chem.*, **2017**, *89*, 5043; (e) H. D. Nelson, S. O. M. Hinterding, R. Fainblat, S. E. Creutz, X. Li, and D. R. J. Gamelin, *J. Am. Chem. Soc.*, **2017**, *139*, 6411; (f) K. E. Knowles, H. D. Nelson, T. B. Kilburn and D. R. Gamelin, *J. Am. Chem. Sci.*, **2015**, *137*, 13138; (g) U. V. Valiev, J. B. Gruber, G. W. Burdick, A. K. Mukhammadiev, D. Fu and V. O. Pelenovich, *Opt. Mater.*, **2014**, *36*, 1101; (h) U. V. Valiev, J. B. Gruber, G. W. Burdick, A. K. Mukhammadiev, D. Fu and V. O. Pelenovich, *J. Lumin*., **2014**, *145*, 393; (i) M. Morita, T. Ozawa, and T. Tsubokura, *J. Lumin*., **1992**, *53*, 495.

5 (a) H. Okada, N. Hara, D. Kaji, M, Shizuma, M. Fujiki and Y. Imai, *Phys. Chem. Chem. Phys*., **2020**. *22*, 13862. (b) D. Kaji, H. Okada, N. Hara. Y. Kondo, S. Suzuki, M. Miyasaka, M. Fujiki and Y. Imai, *Chem. Lett.*, **2020**, *49*, 674.

6 H. Toda, N. Hara, M. Fujiki and Y. Imai, *RSC Adv.*, **2021**, *11*, 1581.

7 (a) J. Kaminský, J. Chalupský, P. Štěpánek, Jan Kříž, and P. Bouř, *J. Phys. Chem. A*, **2017**, *121*, 9064. (b) J-M. Casas-Solvas, T-J. Mooibroek, S. Sandramurthy, J-D. Howgego and A-P. Davis, *Synlett*., **2014**, *25*, 2591. (c) J. G. Foss and M. E. McCarville, *J. Am. Chem. Soi.*, **1967**, 89, 30.

8 (a) L. N. Ferguson, The Modern Structural Theory of Organic Compounds, Prentice-Hall, Upper Saddle River, NJ, 1963; (b) C. Hansch, A. Leo, and R. W. Taft, *Chem. Rev*., **1991**, *91*, 165.